Scientific Research Publishing

Open Journal of Applied Sciences, 2024, 14, 2443-2459
https://www.scirp.org/journal/ojapps
ISSN Online: 2165-3925
ISSN Print: 2165-3917

Isolative Synthesis and Characterization of Cellulose and Cellulose Nanocrystals from *Typha angustifolia*

Lynda S. Mesoppirr[1], Evans K. Suter[1,2], Wesley N. Omwoyo[1,2*], Nathan M. Oyaro[1], Simphiwe M. Nelana[2]

[1]Department of Mathematics and Physical Science, Maasai Mara University, Narok, Kenya
[2]Biotechnology and Chemistry Department, Vaal University of Technology, Vanderbijlpark, South Africa
Email: *wesleyomwoyo@mmarau.ac.ke

How to cite this paper: Mesoppirr, L.S., Suter, E.K., Omwoyo, W.N., Oyaro, N.M. and Nelana, S.M. (2024) Isolative Synthesis and Characterization of Cellulose and Cellulose Nanocrystals from *Typha angustifolia*. *Open Journal of Applied Sciences*, **14**, 2443-2459.
https://doi.org/10.4236/ojapps.2024.149161

Received: July 18, 2024
Accepted: September 8, 2024
Published: September 11, 2024

Abstract

The application potential of cellulosic materials in natural composites and other fields needs to be explored to develop innovative, sustainable, light-weight, functional biomass materials that are also environmentally friendly. This study investigated *Typha angustifolia* (Typha sp.) as a potential new raw material for extracting cellulose nanocrystals (CNCs) for application in wastewater treatment composites. Alkaline treatments and bleaching were used to remove cellulose from the stem fibres. The CNCs were then isolated from the recovered cellulose using acid hydrolysis. The study showed a few distinct functional groups (O-H, -C-H, =C-H and C-O, and C-O-C) in the Fourier Transform Infrared (FTIR) spectra. A scanning electron microscope (SEM) revealed the smooth surface of CPC and CNCs, which resulted from removing lignin and hemicellulose from powdered *Typha angustifolia*. Based on the crystalline index, the powdered *Typha angustifolia*, CPC, and CNCs were 42.86%, 66.94% and 77.41%. The loss of the amorphous section of the Typha sp. fibre resulted in a decrease in particle size. It may be inferred from the features of a Typha sp. CNC that CNCs may be employed as reinforcement in composites for wastewater treatment.

Keywords

Typha angustifolia, Cellulose, Acid Hydrolysis, Chemically Purified Cellulose, Cellulose Nanocrystals

1. Introduction

Cellulose is a widely available, fibre-forming polymer made from universal units.

The units of β-1,4-linked glucopyranose found in cellulose form a naturally occurring linear homopolymer with a high molecular weight [1]. Cellulose consists of three hydroxyl groups that are present in each glucopyranose molecule, giving it properties like biodegradability, biocompatibility, robustness and insolubility in water. It also serves as the protective wall for plant cells. The degree of polymerization in cellulose obtained from wood can reach 10,000 units, but that derived from cotton has 15,000 units [2] [3]. Plant cell walls, such as those found in giant reed, sugarcane bagasse, cotton stalk waste, date seeds, roselle fibres, mengkuang (*Pandanus atrocious*) leaves, waste cotton textiles, and *Typha domingensis* plants, are the primary source of cellulose [3]-[10], eucalyptus hardwood [11]. Other small sources of cellulose include marine creatures (tunicates), algae, bacteria, fungi, and anchovies [12].

Typha is a member of the 30 species-strong Typhaceae family. The genus is known in American English as cattail but in British English as reedmace or bulrush [4]. Wetlands are ideal habitats for the herbaceous grass *Typhaceae angustifolia*. According to Yamauchi *et al.* (2013), the plant is perennial and has rhizomes with a well-developed aerenchyma system, enabling survival in its particular wetland ecosystem [13]. *Typha angustifolia* L. is one of the Typha species that can withstand extremely salinized conditions. It thrives in marshes, fens, meadow grass, and estuaries.

T. angustifolia L. is a macrophyte that may remove harmful metals and toxins by immobilizing them in the sediment and reintroducing them into the earth's geological cycle [13]. In addition, *Typha angustifolia* L. can emit exudates, promote phytovolatilization, carry oxygen into the rhizosphere, and provide donor surfaces that are absorbent and conducive to biofilm formation [14]. Through phytoremediation, *Typha angustifolia* L can eliminate dichloroethane up to 100% for 42 days [15]. Moreover, it may be used as a source of cellulose and to remove methylene blue dye [16] [17]. The plant's high biomass accumulation in its tissues and excellent resilience to stress makes it a popular choice for treating wastewater in wetland environments [18]. However, T. angustifolia L. has not been fully exploited extensively; people frequently overlook and disregard its presence.

Cellulose consists of amorphous and crystalline phases, which are joined together by hydrogen bonds that are both intra- and intermolecular. As a result, heat does not readily break down cellulose [19]. Five distinct polymorphs of cellulose biopolymers are known to exist. Cellulose I to V are examples of cellulose polymorphs. Natural cellulose found in crystallized form is called cellulose I. Subsequently, it can undergo further chemical processing, such as precipitation from the solution or the maceration process (treatment with strong sodium hydroxide solution) to transform it into cellulose II [3].

According to Kumar *et al.* (2010), nanotechnology has become a rapidly expanding multidisciplinary topic of study in the creation of cellulose-based nanocrystals (CNC), cellulose nanowhiskers (CNW), and cellulose nanoparticles (CNP) from easily grown annual plants or agricultural wastes that are readily available locally. Enzymatic hydrolysis, carbon catalyst, and high-pressure homogenization are a

few techniques that may be used to isolate cellulose nanocrystals. Using acids or bases as the hydrolysis solvent in a hydrothermal reactor also catalyzes the molecules into smaller pieces [20]. The amorphous phase of the cellulose may be easily removed by hydrolysis with an acid. The degree of polymerization decreased, producing thicker and shorter crystals [21]. The process involves the assault of loose, amorphous portions of cellulose by hydrogen ions from acids, which breaks the 1,4-glycoside linkages, leaving the crystalline sections of cellulose intact [22]. Following chloride acid hydrolysis, cellulose has a thermal strength of 363.9˚C, more significant than that of sulfate and phosphate acids. It also exhibits a yield of 93.7% and a crystallinity of about 88.6% [23]. In some studies, Date palm seeds were processed into microcrystalline cellulose by Abu-Thabit *et al.* using HCl 2.5 N (1:11 w/v), and a temperature of 85˚C produced a crystalline index of 70% [24].

Acid hydrolysis is often conducted using an ultrasonic method. This method employs a lower temperature for organic compounds, which may boost yield and shorten reaction times, and it has high selectivity. After lignin and hemicellulose are extracted from lignocellulose, the ultrasonic approach helps dissolve the biomass during the separation process of microcrystalline or nanocrystalline cellulose. This method results in a cellulose solution with smaller particle sizes (<0.5 mm), a stable colloid, and easy enzyme accessibility [25].

In this work, the aim was to prepare chemically purified cellulose (CPC) from *Typhacea angustifolia* by the process of dewaxing and delignification using 10% nitic acid and 1M sodium hydroxide and bleaching using Sodium hypochlorite. The prepared CPC were acid hydrolyzed using 32% H_2SO_4 to obtain cellulose nanocrystals.

2. Materials and Methods

2.1. Materials

Typha angustifolia grass was harvested from Maasai Mara University botanical garden, Narok Kenya (1˚41'5.2872"N and 37˚20'27.096"E), altitude of 1827 M above sea level. The grass, about 4 meters tall, was harvested by cutting it, chopped into smaller pieces, washed with distilled water, and air dried in the laboratory (**Figure 1**). It was then ground into fine powder and packed in sealed plastic bags for dewaxing and delignification.

Other chemicals and reagents employed in the study were analytical grade, sodium hydroxide (NaOH ≥ 98%), sulfuric acid (H_2SO_4, >98%), distilled water, sodium hypochlorite (NaOCl, ≥75%), acetic acid (≥99%), and acetone (≥99.9%). The chemicals were purchased from Sigma-Aldrich and were used without further purification.

2.2. Methods

2.2.1. Dewaxing and Delignification

Figures 1a-f illustrate the dewaxing and delignification of *Typha angustifolia* ground powder to obtain cellulose fibres. The dewaxing and delignification began by soaking the dried grass powder in 10% nitric acid; this was aimed at effectively

breaking down lignin, a complex organic polymer in the cell walls of plants that makes them rigid and woody. The soaking temperature was set at 80˚C for 2 hours to achieve this. Similarly, this step also helped in the removal of waxes and other extractives that are not part of the cellulose structure. This step was followed by thorough washing with deionized water to remove residual acid and dissolved components. Following this, the material underwent alkaline pre-treatment with 1.0M sodium hydroxide (NaOH); this was aimed at breaking down hemicellulose and residual lignin further that were still present after the acid treatment. The resulting cellulose fibres were then quenched with cold deionized water and washed until a neutral pH. This step was performed to ensure that the material was ready for the subsequent purification without any chemical residues that might interfere with further treatments.

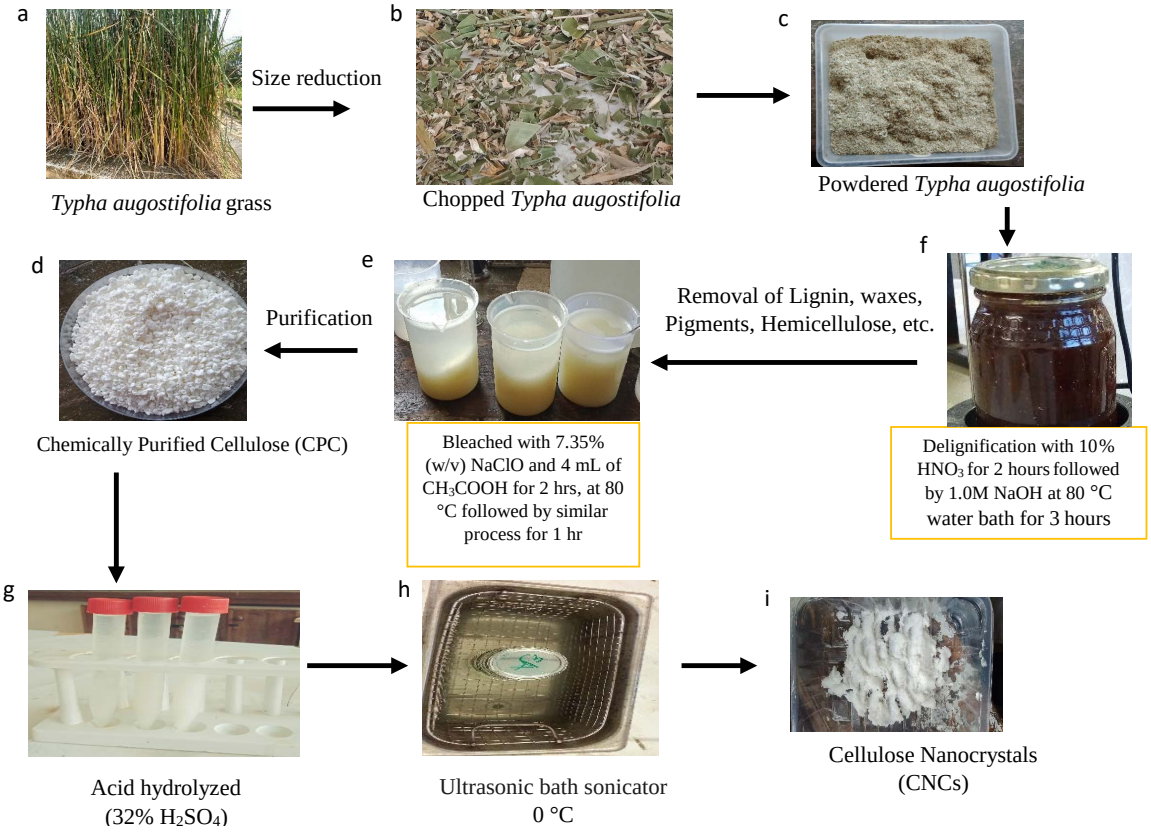

Figure 1. Summarized schematic diagram for CPC isolation and synthesis of CNCs.

2.2.2. Chemical Purification (Bleaching)

The chemical bleaching process and the resultant chemically purified cellulose are shown in **Figures 1e-d**. The obtained cellulose fibres were refluxed with 350 mL (7.35% (w/v)) sodium hypochlorite, 2% (w/v), followed by 4 mL acetic acid. The reaction mixture was agitated for 3 hours at 80˚C with constant stirring at 900 rpm. The sodium hypochlorite, a strong oxidizing agent, aided in the breakdown of pigments and impurities like lignin. Acetic acid was added to improve the bleaching effect and regulate the pH. The resultant chemically refined cellulose was next

filtered using a Büchner funnel attached to a vacuum pump to separate the liquid phase from the solid cellulose effectively. The chemically purified cellulose was further washed to remove any remaining contaminants. The washing was thoroughly performed with deionized water until it achieved a neutral pH. Further purification was made by using acetone in a Soxhlet chamber to effectively remove organic impurities such as waxes and lipids. The process of soxhlet extraction allowed for constant washing with fresh acetone. This was then followed by three days of room-temperature drying to ensure that the CPC was free of acetone. The resulting pure cellulose was kept for characterization and further experiments.

2.2.3. Synthesis of Nanocellulose

Figures 1g-i illustrate a schematic process for synthesizing CNCs through acid hydrolysis. Briefly, in a 500 mL conical flask, 20 g of chemically purified cellulose (CPC) was combined with 400 mL (32% w/v) sulfuric acid. The synthesis process involved using a 1:20 (g:mL) cellulose-to-acid ratio; the mixture was heated in a water bath for 45 minutes. The solution was first heated to 45˚C, then to 55˚C with constant stirring at 600 rpm. The hydrolysis process was stopped by carefully quenching it with 200 mL of 10-fold deionized water five times. The resultant suspension was homogenized using a centrifuge for 40 minutes at 10,000 rpm. This process was repeated five times, each time removing the supernatant from the sediment and replacing it with new distilled water until the supernatant's pH was neutral. After three days of room temperature drying, the resulting CNCs were packaged for characterization.

2.3. Characterization

2.3.1. Fourier Transform Infrared (FTIR) Analysis

The functional groups in the *Typha angustifolia* grass powder, chemically purified cellulose, and nanocellulose were determined using a Thermo Scientific Nicolet iS10 (Smart iTR) FTIR spectrometer with a diamond-based ATR compartment. The spectral resolution was set to 4 cm^{-1} over a 4000 and 500 cm^{-1} wavelength range. An average of 16 scans were captured for each spectrum, and the primary absorption peaks were identified.

2.3.2. X-Ray Diffraction (XRD) Analysis

The XRD pattern and degree of crystallinity of *Typha angustifolia* grass powder, CPC, and CNCs were assessed using a Siemens D5000 X-ray diffractometer at room temperature. A monochrome step scanner Cu-K radiation set at a wavelength of 0.1538 nm was used to scan the samples with a 2θ from 10˚ to 80˚ scan angles, and 0.02 and 5.0 min scanning times. The crystallinity index (C_rI) was calculated using Equation (1) below.

$$\text{Crystal size}\left(D\right)=\frac{K\lambda}{\beta\,\text{Cos}\,\theta} \tag{1}$$

where I_{002} and I_{am} represent the intensity of the peak of crystalline and amorphous

regions, the Scherrer Equation (2) was used empirically for the crystal methods' size.

$$C_r I(\%) = \frac{I_{002} - I_{am}}{I_{002}} \times 100 \quad (2)$$

From the equation, the crystal structure has a K factor of 0.89, λ is the length of a light wave (1.54056 Å), β is the Full Width at Half Maximum (FWHM) in radians, and θ is the angle of diffraction in degrees.

2.3.3. Scanning Electron Microscope-Electron Dispersive Spectroscopy (SEM-EDS) Analysis

The surface morphology of *Typha angustifolia* grass powder, CPC, and CNCs was examined using a scanning electron microscope (JEOL-IT 7500LA, Japan) with an accelerating voltage of 15 - 20 kV. The samples were sputtered with a thin coating of gold metal after being placed on a carbon tape metal stub. Electron dispersive spectroscopy (EDS) (JSM-IT500, JEOL Ltd., Tokyo, Japan) was used for elemental analysis to determine the percentage purity of the samples.

2.3.4. Thermogravimetric (TGA) Analysis

TGA was used to quantify the mass loss for the *Typha angustifolia* grass powder, CPC, and CNCs under a controlled temperature change in a nitrogen atmosphere. Approximately 18.00 mg samples were examined using a Mettler Toledo Thermogravimetric analyzer linked to an inert nitrogen gas flow and pyrolyzed at 10˚C/min from 30˚C to 1000˚C.

3. Results and Discussions

3.1. Physical Appearance

Figures 2a-d depicts the physical characteristics of the raw chopped *Typha angustifolia* as collected from the field without any chemical treatments, the powdered *Typha angustifolia*, and the chemically purified cellulose before and after acid hydrolysis. The chemical alteration caused the *Typha angustifolia* to become whiter in colour. The raw and powdered *Typha angustifolia* were green and brown, as seen in **Figure 2a** and **Figure 2b**. The cellulose (white powder) was formed by treating *Typha angustifolia* powder with HNO_3, NaOH, and sodium hypochlorite (**Figure 1c**). Whiter and gel, hairy-like material (cellulose nanocrystals) was obtained by hydrolyzing the recovered cellulose with H_2SO_4 acid and then washing it with acetone (**Figure 2d**). Similar results were obtained by Evans *et al.* (2019), who isolated cellulose from sugar cane bagasse and then synthesized cellulose nanocrystals from it through acid hydrolysis [9]. This established that chemical treatment with NaOH and purification (bleaching with (NaClO) makes the fibre change colour. In a different research, Johar *et al.* (2012) treated rice husk fibres at various stages and observed and described their physical and chemical characteristics. When the rice husk was treated with an alkaline solution, it lost its brown colour and became entirely white [26]. The observed changes were all associated with eliminating wax and pigments like chlorophyll, lignin, hemicellulose, etc. [21].

Figure 2. Physical appearance of (a) Chopped *Typha angustifolia*, (b) Crushed *Typha angustifolia*, (c) Isolated cellulose and (d) Cellulose nanocrystals.

3.2. Functional Group Analysis (FTIR)

The functional groups for the *Typha angustifolia*, chemically purified cellulose and cellulose nanocrystals are illustrated in **Figure 3**. The major absorption bands corresponding to different groups for the grass material to the nanocellulose were observed from 500 cm^{-1} to around 3600 cm^{-1}. The broad peak at around 3309 cm^{-1} is linked to intramolecular hydrogen bond O-H stretching, as seen in all the materials. Similarly, all materials exhibit the C-H stretching of the cellulosic materials, with only minor shifts and variations in intensity, at peaks around 2892 and 2915 cm^{-1} [27]. The wavenumber around 898 cm^{-1} is attributed to all materials' C-H rocking vibration of cellulose. The bands at 1034 cm^{-1}, 1730 cm^{-1} and 1632 cm^{-1} are due to C-O-C of the pyranose ring, carboxyl groups found in esters and acids that are primarily found in lignin and O-H bending vibrations, respectively [11] [28]. The peak at 1730 cm^{-1} was only observed in the *Typha angustifolia* grass powder due to the esters and acids only present in the lignin. The peak was not seen in CPC and CNC samples, which is a clear indication that the esters and acids were successfully removed. At around 1157 cm^{-1}, a peak of O-H associated with C-O-H was present and was more extensive and more well-defined in cellulose than the rest of the samples, indicating a purer sample [28]. The O-H peak associated with absorbed water at around 1632 cm^{-1} was constant for all the samples.

The major difference between the grass sample and the cellulosic materials was noted at around 1245 cm^{-1}; this peak is attributed to C=C of aromatic rings, an indication of a mixture of other organic compounds, aromatic in nature, found in plants' matrix-like phenols and lignin. The peak was not present in the delignified grass and the chemically purified cellulose, indicating that lignin and all the other compounds were removed entirely.

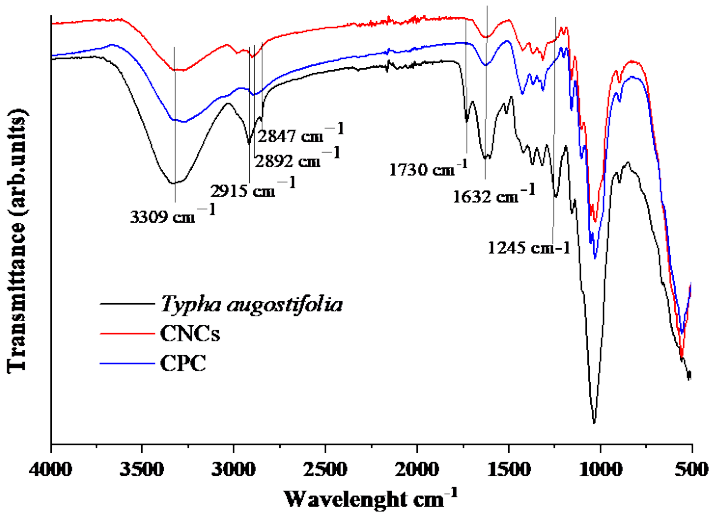

Figure 3. FTIR spectra of *Typha angustifolia*, CPC, and CNCs.

3.3. Scanning Electron Microscopy (SEM)

The structure and diameter of the CPC and CNCs were determined by scanning electron microscopy, and the results are presented in **Figures 4a-c**. From the SEM images, the *Typha angustifolia* displays regular rod-like structures that are not chemically connected with spongy-like and loose materials stuck on its rough surface, indicating that the materials are of different composition (**Figure 4a**). On dewaxing and delignification, it is seen that the CPC structures are not fused despite having a lengthy, uneven form (**Figure 4b**). The smooth surface of the cellulose could have resulted from lignin and hemicellulose extracted from the powdered *Typha angustifolia* [29]. The amorphous and crystalline portions of microcrystalline cellulose are still fused, resembling a continuous thread. The cellulose had the same form as the other references [3] [14] [30]. Meanwhile, after H_2SO_4 hydrolysis, CNCs (**Figure 4c**) demonstrate that only crystalline regions remain since H_2SO_4 breaks down the amorphous regions. The size of the powdered *Typha angustifolia*, the chemically purified cellulose was 271.67 ± 3.02 μm, 161.15 ± 3.83 μm, and 98.57 ± 2.54 nm before and after hydrolysis.

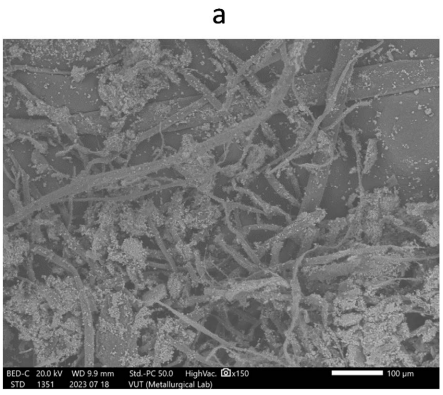

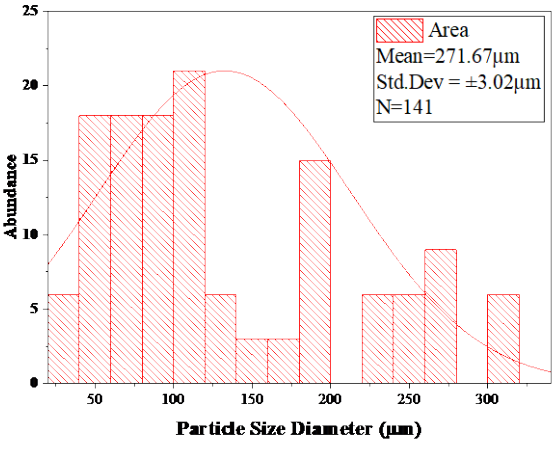

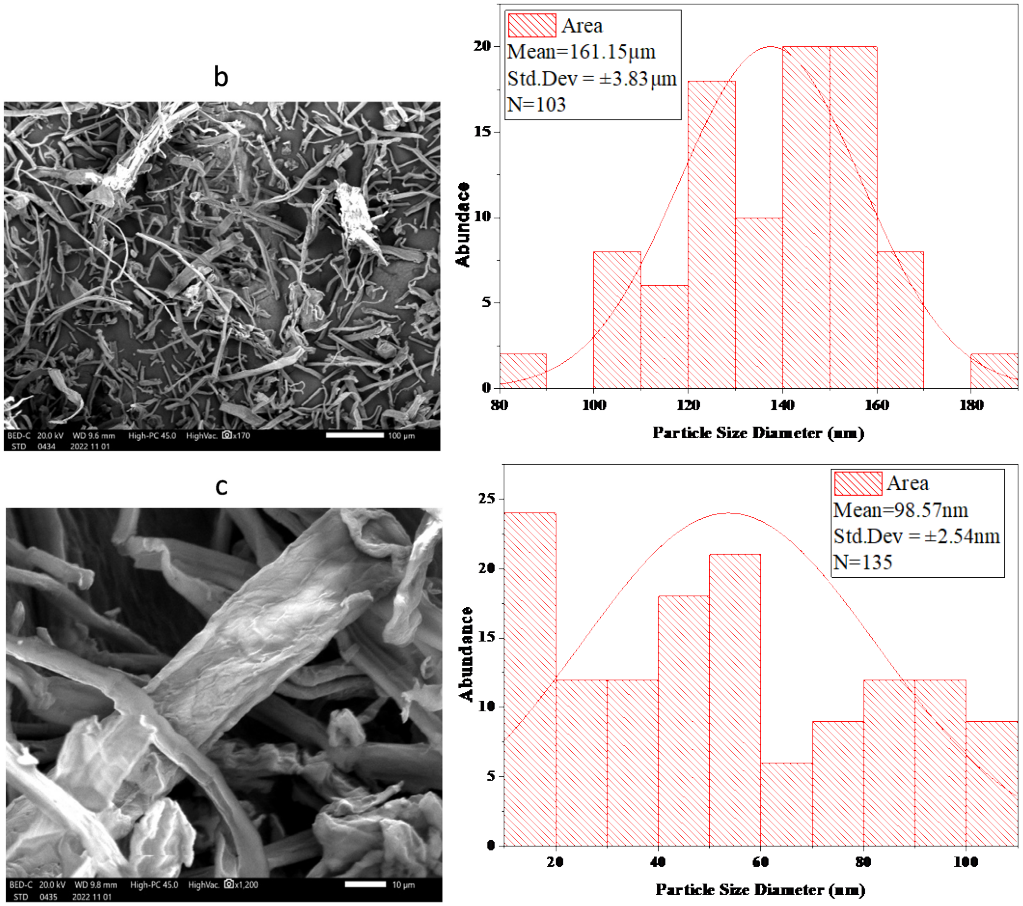

Figure 4. Scanning electron (SEM) images for: (a) *Typha angustifolia*; (b) CPC; (c) CNCs.

3.4. Elemental Analysis

The quantification of the composition of elements present in the *Typha angustifolia*, the prepared cellulosic materials done using Electron Diffraction Spectroscopy (EDS) is shown in **Figures 5a-c**. The analysis was performed to investigate further the composition of the isolated cellulose and the synthesized CNCs (**Figure 5b** and **Figure 5c**). From the *Typha angustifolia* EDS spectrum, C and O, the main building blocks of cellulose, were quantified to be 51.60% ± 0.13% and 48.35% ± 0.27%. While traces of Ca and Fe were found to be 0.04% ± 0.01% and 0.01% ± 0.01%, respectively. The trace elements could be attributed to nutrients in the *Typha angustifolia* grass. However, for the cellulosic materials, carbon and oxygen atoms constituted 52.29% ± 0.23% and 47.71% ± 0.46% for CPC and 59.75% ± 0.18% and 40.25% ± 0.35% for CNCs. The elemental analysis showed that the purity of the cellulose was purely formed of carbons and oxygen. On H_2SO_4 hydrolysis, it noted that there is an increase in C percentage with a decrease in that of O. Studies indicate that the breakdown of cellulose into smaller components (cellulose nanocrystals) results in the removal of oxygen-containing functional groups [31]. This further confirmed that the isolation of cellulose and the synthesis of its nanocrystals was successfully achieved.

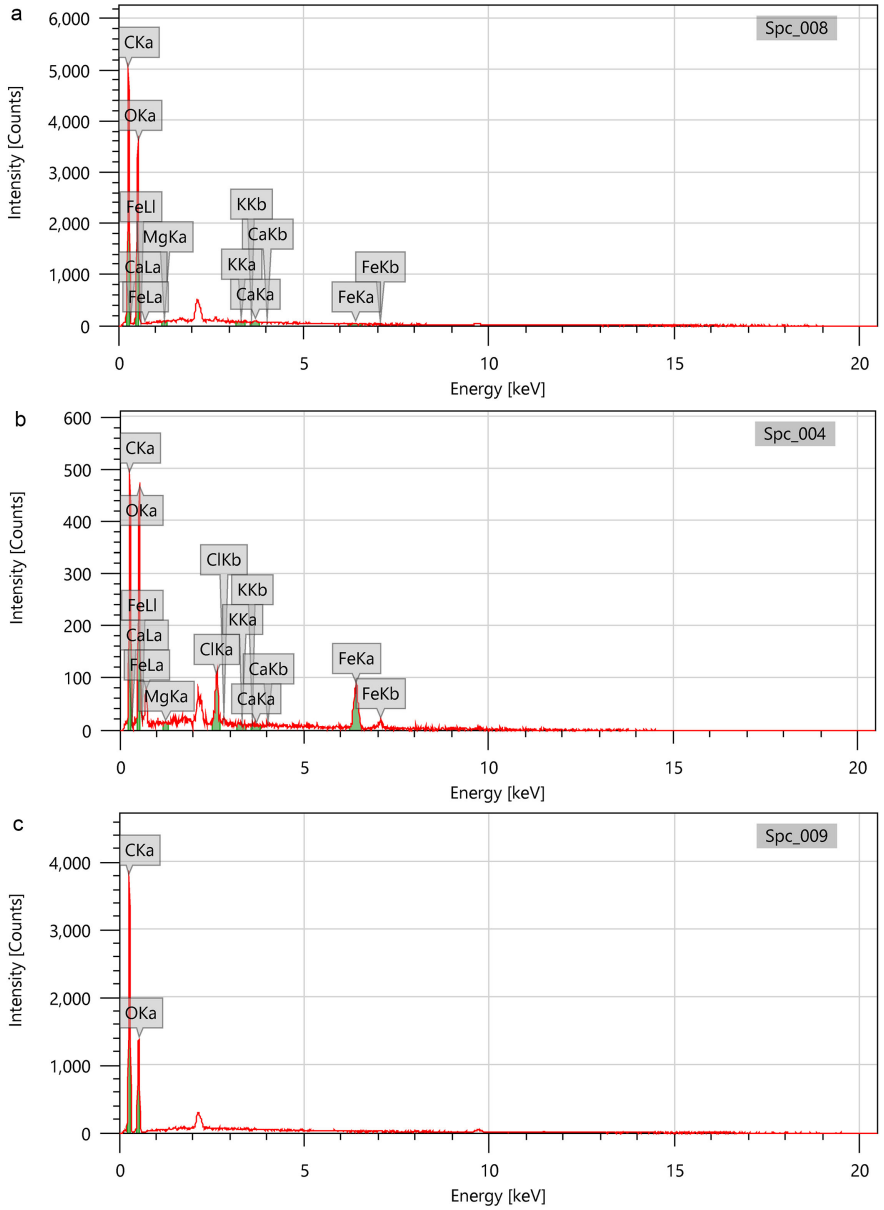

Figure 5. EDS spectrum of *Typha angustifolia*, CPC, and CNCs.

3.5. Crystalline Structure Analysis X-Ray Diffraction

Figure 6 shows the crystal structures, while **Table 1** shows the crystallinity indices of *Typha angustifolia* powder, CPC and CNCs. While the peaks in each sample varied in intensity, they all displayed similar patterns except for *Typha angustifolia* grass powder. Cellulose polymorphs I and II correspond to either CNCs or CPC. High amounts of NaOH added to *Typha angustifolia* grass powder changed the cellulose properties from cellulose I to cellulose II. The (101) crystalline planes of hemicellulose are thought to be responsible for the first XRD peak [32]. The (002) planes from the monoclinic structure of cellulose I are referred to as the second peak [33]. Similarly, the third XRD reflex, which appears as a blurred band, confirms the presence of the (040) crystal faces from the amorphous areas

(primarily lignin and hemicellulose). It is reported that for cellulose I and cellulose II, the peak intensity values of crystal cellulose are $2\theta = 22.5^{\circ}$ and $2\theta = 20.1^{\circ}$, respectively. The highest intensity value of amorphous cellulose is $2\theta = 18^{\circ}$ for cellulose I and $2\theta = 16.3^{\circ}$ for cellulose II [29]. From **Figure 4a**, the cellulose's post-hydrolysis peak pattern shows that crystalline cellulose I have a typical structure on the peak of 2θ at 22.64˚. In contrast, amorphous cellulose II has a typical structure on the peak of 2θ at 15.83˚. Crystalline cellulose II and crystalline cellulose I showed peaks at intensity values of 2θ of 16.23˚ and 22.58˚, respectively, before hydrolysis of cellulose. The powdered *Typha angustifolia* showed peaks with intensity values of 2θ of 16.11˚, 21.00˚, and 22.89˚ representing amorphous cellulose I, amorphous cellulose II, and crystalline cellulose II [29] [34].

Table 1. Crystallinity indices of *Typha angustifolia* grass powder, CPC, and CNCs.

Sample	$2\theta_{(Amorphous)}$ (˚)		$2\theta_{(002)}$ (˚)		Crystallinity Index (C_rI%)
	Degree	Intensity, I_{am}	Degree	Intensity, I_{002}	
Typha angustifolia	21.00	376	34.97	658	42.86
CPC	22.58	287	34.73	868	66.94
CNCs	22.64	211	34.84	934	77.41

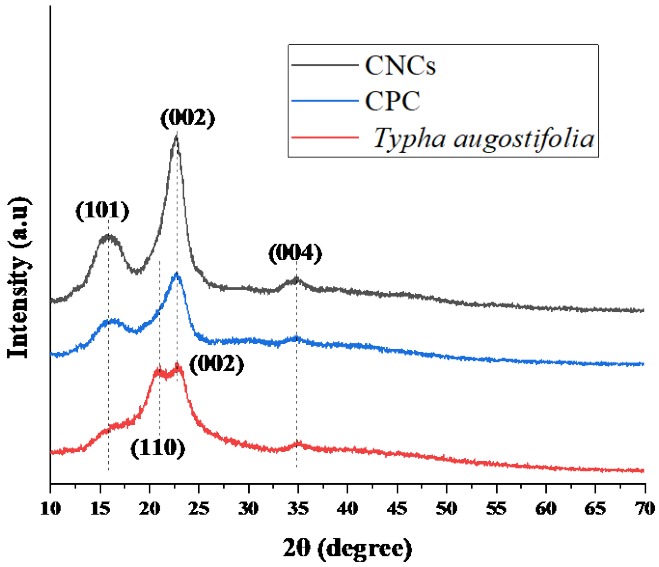

Figure 6. XRD pattern of *Typha angustifolia*, CPC, and CNCs.

Following hydrolysis, the crystallinity of CNCs is better than that of CPC and *Typha angustifolia*. It is evident from each sample's peak intensity. Additionally, it is evident from the peak heights of each sample that cellulose has a more significant peak upon hydrolysis than the others. Based on the crystalline index and the size of the powdered *Typha angustifolia*, the cellulose microcrystalline was 42.86% and 308.3 μm, 66.94% and 280.9 μm, and 77.41% and 87.3 nm before and after hydrolysis.

3.6. Thermal Analysis

Figure 7a and Figure 7b with Table 2 provides TGA/DTG data from the thermal degradation mechanisms of powdered *Typha angustifolia*, CPC, and CNCs. The breakdown of hemicellulose happens between 200˚C - 260˚C, lignin at 280˚C - 500˚C, and cellulose at 340˚C - 350˚C, according to Adewale *et al.* (2022) [35]. The TGA and DTG curves for the samples shown in Figure 7a and Figure 7b display two main peaks for CPC and CNCs, while *Typha angustifolia* displays three. For all three samples, the emission of water, volatile chemicals, polysaccharides, and other low molecular weight molecules peaked between 70˚C and 150˚C [9] [29]. For CPC, CNCs, and *Typha angustifolia* powder, the percentage weight loss from the first peak in that temperature range was 8.31%, 8.98%, and 14.23%, respectively. The information demonstrated that *Typha angustifolia* powder still had a greater water content than the other samples. The existence of an absorption band at a peak of 1630 cm^{-1} from the FTIR data on the water's hydrogen bond supports this. The second peak, which ranges from 250˚C to 350˚C, indicates the presence of cellulose degradation, which indicates polymer and carboxylate elimination, dehydration, and glycosyl breakdown. The second peak's weight loss data was found to be 68.76% of the CNCs, 44.62% of the CPC, and 35.04% of the powdered *Typha angustifolia*. The final degradation indicates an oxidation process and residue breakdown, which is located between 400˚C and 1000˚C. The final degradation weight loss for powdered *Typha angustifolia* powder was 14.29%, CPC was 2.16%, and CNCs was 2.68%. *Typha angustifolia* powder has higher heat degradation, as the TGA and DTG curves indicate. It is reported that the benzene ring of the aromatic polycyclic structure of lignin, hemicellulose, and other non-cellulose molecules may contribute to this [24]. Compared to CPC and CNCs, *Typha angustifolia* powder in Table 2 has the lowest thermal stability, even though CNCs take the longest decomposing time. It starts to break down at 229.28˚C. The increased thermal stability resulting from applying H2SO4 in acid hydrolysis treatment can cause this [30].

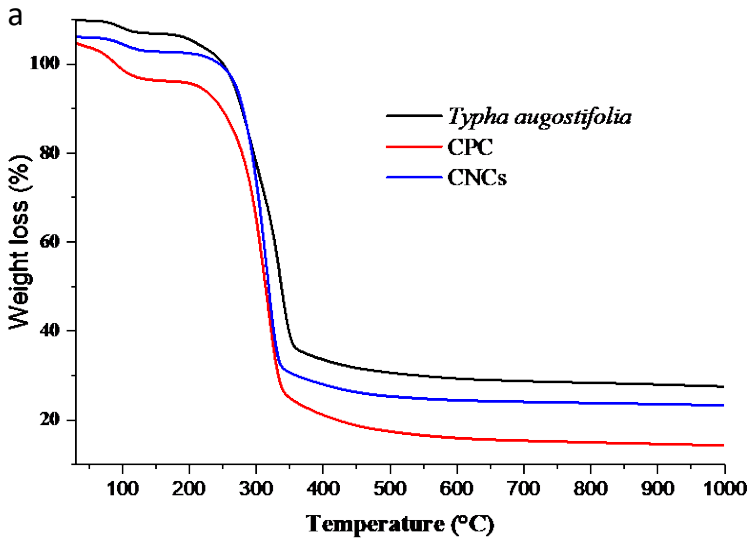

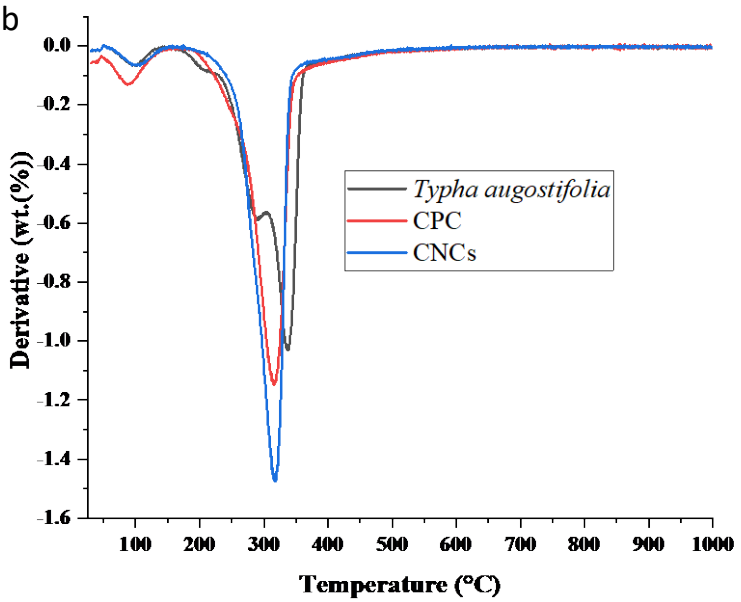

Figure 7. (a) TGA and (b) DTG curve of *Typha angustifolia*, CPC, and CNCs.

Table 2. Thermal characteristics of *Typha angustifolia* grass powder, CPC and CNCs.

Temperature	CPC (˚C)	CNCs (˚C)	*Typha angustifolia* (˚C)
Tonset	253.24	239.01	229.28
Tendset	339.56	344.45	354.06
Td	315.19	315.18	298.32

Following hydrolysis, there was a more significant amount of cellulose residue. This might happen when H_2SO_4 is added during the acid hydrolysis procedure. Breakdown of the cellulose polymer: β-1,4-glycosidic linkages, followed by the generation of levoglucosan and charcoal, was seen at higher temperatures for *Typha angustifolia* powder, CPC and CNCs [30].

4. Conclusion

The research established that cellulose can be isolated from *Typha angustifolia*. The removal of non-cellulosic materials can be improved through dewaxing and delignification. From the XRD data, the crystallinity of the nanocrystals increased, indicating that the crystalline phase was exposed after the hemicelluloses and lignin, as well as other organic and inorganic components, were successfully eliminated. The particle size decreased considerably in diameter after acid hydrolysis of cellulose, as revealed by XRD, indicating better CNC characteristics. The findings further suggest that *Typha angustifolia*, a perennial plant with rhizomes with a well-developed aerenchyma system enabling survival in its particular wetland ecosystem, can be employed in the extensive production of cellulosic materials.

Acknowledgements

The authors are thankful to Maasai Mara University for offering laboratory space.

The Vaal University of Technology is for FTIR and SEM-EDS analysis, and North West University is for the TGA analysis. The University of Witwatersrand, South Africa, for XRD analysis.

Authors' Contributions

Miss. Lynda Mesoppirr collected the samples, ran the experiments, and wrote the manuscript.

Mr. Evans Suter assisted in sample characterization and proofread the draft article.

Dr. Wesley Omwoyo provided the chemicals, coordinated sample characterization, and proofread the draft article.

Prof. N.M. Oyaro was involved in the article development, data analysis, and proofreading.

Dr. Simphiwe Nelana coordinated sample characterization at Vaal University of Technology, Northwest University and the University of Witwatersrand, all in South Africa.

Data Availability

This article includes all the data generated or analyzed during this study.

Conflicts of Interest

The authors declare no conflicts of interest regarding the publication of this paper.

References

[1] Ghanbarzadeh, B. and Almasi, H. (2013) Biodegradable Polymers. In: Chamy, R. and Rosenkranz, F., Eds., *Biodegradation-Life of Science*, InTech, 141-185. https://doi.org/10.5772/56230

[2] Siqueira, G., Bras, J. and Dufresne, A. (2010) Cellulosic Bionanocomposites: A Review of Preparation, Properties and Applications. *Polymers*, **2**, 728-765. https://doi.org/10.3390/polym2040728

[3] Trache, D., Hussin, M.H., Hui Chuin, C.T., Sabar, S., Fazita, M.R.N., Taiwo, O.F.A., *et al.* (2016) Microcrystalline Cellulose: Isolation, Characterization and Bio-Composites Application—A Review. *International Journal of Biological Macromolecules*, **93**, 789-804. https://doi.org/10.1016/j.ijbiomac.2016.09.056

[4] Pandey, A. and Verma, R.K. (2018) Taxonomical and Pharmacological Status of Typha: A Review. *Annals of Plant Sciences*, **7**, 2101-2106. https://doi.org/10.21746/aps.2018.7.3.2

[5] Barragán, E.U.P., Guerrero, C.F.C., Zamudio, A.M., Cepeda, A.B.M., Heinze, T. and Koschella, A. (2019) Isolation of Cellulose Nanocrystals from Typha Domingensis Named Southern Cattail Using a Batch Reactor. *Fibers and Polymers*, **20**, 1136-1144. https://doi.org/10.1007/s12221-019-8973-1

[6] Kian, L.K., Jawaid, M., Ariffin, H. and Alothman, O.Y. (2017) Isolation and Characterization of Microcrystalline Cellulose from Roselle Fibers. *International Journal of Biological Macromolecules*, **103**, 931-940. https://doi.org/10.1016/j.ijbiomac.2017.05.135

[7] Li, M., He, B. and Zhao, L. (2019) Isolation and Characterization of Microcrystalline Cellulose from Cotton Stalk Waste. *BioResources*, **14**, 3231-3246. https://doi.org/10.15376/biores.14.2.3231-3246

[8] Tlou, S., Suter, E., Alfred, M., Rutto, H. and Omwoyo, W. (2023) *In situ* Capping of Silver Nanoparticles with Cellulosic Matrices from Wheat Straws in Enhancing Their Antimicrobial Activity: Synthesis and Characterization. *Journal of Environmental Science and Health*, *Part A*, **58**, 903-913. https://doi.org/10.1080/10934529.2023.2260295

[9] Evans, S.K., Wesley, O.N., Nathan, O. and Moloto, M.J. (2019) Chemically Purified Cellulose and Its Nanocrystals from Sugarcane Baggase: Isolation and Characterization. *Heliyon*, **5**, e02635. https://www.cell.com/heliyon/pdf/S2405-8440(19)36295-4.pdf https://doi.org/10.1016/j.heliyon.2019.e02635

[10] Jacob Rani, B.S. and Venkatachalam, S. (2022) A Neoteric Approach for the Complete Valorization of Typha Angustifolia Leaf Biomass: A Drive Towards Environmental Sustainability. *Journal of Environmental Management*, **318**, Article 115579. https://doi.org/10.1016/j.jenvman.2022.115579

[11] Zhang, J. and Zou, W. (2019) A Novel Method for Isolating Nanocrystalline Cellulose from Eucalyptus Hardwood. *Journal of Analytical Sciences*, *Methods and Instrumentation*, **9**, 51-62. https://doi.org/10.4236/jasmi.2019.93006

[12] Ismail, M.M., Elkomy, R.G. and El-Sheekh, M.M. (2023) Bioactive Compounds from Components of Marine Ecosystem. In: Takahashi, T., Eds., *Marine Ecology*: *Current and Future Developments*, Bentham Science Publishers, 206-256. https://doi.org/10.2174/9789815051995123030009

[13] Yamauchi, T., Shimamura, S., Nakazono, M. and Mochizuki, T. (2013) Aerenchyma Formation in Crop Species: A Review. *Field Crops Research*, **152**, 8-16. https://doi.org/10.1016/j.fcr.2012.12.008

[14] Patro, A., Dwivedi, S., Panja, R., Saket, P., Gupta, S., Mittal, Y., *et al.* (2023) Constructed Wetlands for Wastewater Management. In: Aryal, N., Zhang, Y., Patil, S.A. and Pant, D., Eds., *Material-Microbes Interactions*, Academic Press, 315-348. https://doi.org/10.1016/b978-0-323-95124-1.00018-8

[15] Al-Baldawi, I.A. (2018) Removal of 1,2-Dichloroethane from Real Industrial Wastewater Using a Sub-Surface Batch System with *Typha angustifolia* L. *Ecotoxicology and Environmental Safety*, **147**, 260-265. https://doi.org/10.1016/j.ecoenv.2017.08.022

[16] Namasivayam, S.K.R., Prakash, P., Babu, V., Paul, E.J., Bharani, R.S.A., Kumar, J.A., *et al.* (2023) Aquatic Biomass Cellulose Fabrication into Cellulose Nanocomposite and Its Application in Water Purification. *Journal of Cleaner Production*, **396**, Article 136386. https://doi.org/10.1016/j.jclepro.2023.136386

[17] Amri, A.E., Bensalah, J., Idrissi, A., Lamya, K., Ouass, A., Bouzakraoui, S., *et al.* (2022) Adsorption of a Cationic Dye (Methylene Bleu) by Typha Latifolia: Equilibrium, Kinetic, Thermodynamic and DFT Calculations. *Chemical Data Collections*, **38**, Article 100834. https://doi.org/10.1016/j.cdc.2022.100834

[18] Ievinsh, G. (2023) Halophytic Clonal Plant Species: Important Functional Aspects for Existence in Heterogeneous Saline Habitats. *Plants*, **12**, Article 1728. https://doi.org/10.3390/plants12081728

[19] Wulandari, W.T., Rochliadi, A. and Arcana, I.M. (2016) Nanocellulose Prepared by Acid Hydrolysis of Isolated Cellulose from Sugarcane Bagasse. *IOP Conference Series*: *Materials Science and Engineering*, **107**, Article 012045. https://doi.org/10.1088/1757-899x/107/1/012045

[20] Kumar, S., Negi, Y.S. and Upadhyaya, J.S. (2010) Studies on Characterization of Corn Cob Based Nanoparticles. *Advanced Materials Letters*, **1**, 246-253.

[21] Trache, D., Hussin, M.H., Haafiz, M.K.M. and Thakur, V.K. (2017) Recent Progress in Cellulose Nanocrystals: Sources and Production. *Nanoscale*, **9**, 1763-1786. https://doi.org/10.1039/c6nr09494e

[22] Yeasmin, S. (2016) A Study of Acid Hydrolysis Based Synthesis of Microcrystalline and Nano-Crystalline Cellulose from Local Lignocellulosic Materials. https://api.semanticscholar.org/CorpusID:201044441

[23] Hokkanen, S., Bhatnagar, A. and Sillanpää, M. (2016) A Review on Modification Methods to Cellulose-Based Adsorbents to Improve Adsorption Capacity. *Water Research*, **91**, 156-173. https://doi.org/10.1016/j.watres.2016.01.008

[24] Abu-Thabit, N.Y., Judeh, A.A., Hakeem, A.S., Ul-Hamid, A., Umar, Y. and Ahmad, A. (2020) Isolation and Characterization of Microcrystalline Cellulose from Date Seeds (*Phoenix dactylifera* L.). *International Journal of Biological Macromolecules*, **155**, 730-739. https://doi.org/10.1016/j.ijbiomac.2020.03.255

[25] Guo, J., Guo, X., Wang, S. and Yin, Y. (2016) Effects of Ultrasonic Treatment during Acid Hydrolysis on the Yield, Particle Size and Structure of Cellulose Nanocrystals. *Carbohydrate Polymers*, **135**, 248-255. https://doi.org/10.1016/j.carbpol.2015.08.068

[26] Johar, N., Ahmad, I. and Dufresne, A. (2012) Extraction, Preparation and Characterization of Cellulose Fibres and Nanocrystals from Rice Husk. *Industrial Crops and Products*, **37**, 93-99. https://doi.org/10.1016/j.indcrop.2011.12.016

[27] Dantas, P.A. and Botaro, V.R. (2012) Synthesis and Characterization of a New Cellulose Acetate-Propionate Gel: Crosslinking Density Determination. *Open Journal of Polymer Chemistry*, **2**, 144-151. https://doi.org/10.4236/ojpchem.2012.24019

[28] Suter, E.K., Rutto, H.L., Seodigeng, T.S., Kiambi, S.L. and Omwoyo, W.N. (2024) Green Isolation of Cellulosic Materials from Recycled Pulp and Paper Sludge: A Box-Behnken Design Optimization. *Journal of Environmental Science and Health, Part A*, **59**, 64-75. https://doi.org/10.1080/10934529.2024.2331942

[29] Tarchoun, A.F., Trache, D., Klapötke, T.M., Derradji, M. and Bessa, W. (2019) Eco-friendly Isolation and Characterization of Microcrystalline Cellulose from Giant Reed Using Various Acidic Media. *Cellulose*, **26**, 7635-7651. https://doi.org/10.1007/s10570-019-02672-x

[30] Adawiyah, R., Suryanti, V. and Pranoto, (2022) Preparation and Characterization of *Microcrystalline cellulose* from Lembang (*Typha angustifolia* L.). *Journal of Physics: Conference Series*, **2190**, Article 012007. https://doi.org/10.1088/1742-6596/2190/1/012007

[31] Khili, F., Borges, J., Almeida, P.L., Boukherroub, R. and Omrani, A.D. (2018) Extraction of Cellulose Nanocrystals with Structure I and II and Their Applications for Reduction of Graphene Oxide and Nanocomposite Elaboration. *Waste and Biomass Valorization*, **10**, 1913-1927. https://doi.org/10.1007/s12649-018-0202-4

[32] Guna, V., Ilangovan, M., Adithya, K., Akshay Koushik, C.V., Srinivas, C.V., Yogesh, S., *et al.* (2019) Biofibers and Biocomposites from Sabai Grass: A Unique Renewable Resource. *Carbohydrate Polymers*, **218**, 243-249. https://doi.org/10.1016/j.carbpol.2019.04.085

[33] Cheikh Rouhou, M., Abdelmoumen, S., Thomas, S., Attia, H. and Ghorbel, D. (2018) Use of Green Chemistry Methods in the Extraction of Dietary Fibers from Cactus Rackets (*Opuntia ficus indica*): Structural and Microstructural Studies. *International Journal of Biological Macromolecules*, **116**, 901-910. https://doi.org/10.1016/j.ijbiomac.2018.05.090

[34] Chilukoti, G.R. and Mandapati, R.N. (2020) Characterization of Cellulosic Leaf Fiber from the Typha Angustifolia Plant. *Journal of Natural Fibers*, **19**, 2516-2526. https://doi.org/10.1080/15440478.2020.1819511

[35] Adeniyi, A.G., Adeyanju, C.A., Emenike, E.C., Otoikhian, S.K., Ogunniyi, S., Iwuozor, K.O., *et al.* (2022) Thermal Energy Recovery and Valorisation of *Delonix regia* Stem for Biochar Production. *Environmental Challenges*, **9**, Article 100630. https://doi.org/10.1016/j.envc.2022.100630